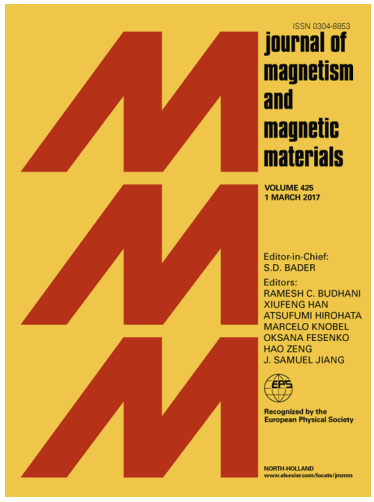

Rod-like particles of silica-coated maghemite: synthesis via akaganeite, characterization and biological properties

Pavel Veverka, Mariia Pashchenko, Lenka Kubí čková, Jarmila Kuličková, Zdeněk Jirák, Radim Havelek, Karel Královec, Jaroslav Kohout, Ondřej Kaman

PII: S0304-8853(18)32500-9
DOI: https://doi.org/10.1016/j.jmmm.2018.12.037
Reference: MAGMA 64728

To appear in: *Journal of Magnetism and Magnetic Materials*

Received Date: 9 August 2018
Revised Date: 5 December 2018
Accepted Date: 10 December 2018

Please cite this article as: P. Veverka, M. Pashchenko, L. Kubí čková, J. Kuličková, Z. Jirák, R. Havelek, K. Královec, J. Kohout, O. Kaman, Rod-like particles of silica-coated maghemite: synthesis via akaganeite, characterization and biological properties, *Journal of Magnetism and Magnetic Materials* (2018), doi: https://doi.org/10.1016/j.jmmm.2018.12.037

Rod-like particles of silica-coated maghemite: synthesis via akaganeite, characterization and biological properties

Pavel Veverka[1], Mariia Pashchenko[1], Lenka Kubíčková[1,2], Jarmila Kuličková[1], Zdeněk Jirák[1], Radim Havelek[3], Karel Královec[3,4], Jaroslav Kohout[2] and Ondřej Kaman[1]*

[1] *Institute of Physics, Czech Academy of Sciences, Cukrovarnická 10, 162 00 Praha 6, Czech Republic*
[2] *Faculty of Mathematics and Physics, Charles University, V Holešovičkách 2, 180 00 Praha 8, Czech Republic*
[3] *Faculty of Medicine in Hradec Králové, Charles University, Šimkova 870, 500 38 Hradec Králové, Czech Republic*
[4] *Faculty of Chemical Technology, University of Pardubice, Studentská 573, 532 10 Pardubice, Czech Republic*

*Corresponding author: kamano@seznam.cz, Tel.: +420 220 318 420

Keywords

Magnetic nanoparticles, Magnetic nanorods, Solvothermal procedure, Mössbauer spectroscopy, Cytotoxicity

Abstract

A multistep procedure, employing akaganeite FeO(OH,Cl) as a precursor, was developed for the preparation of rod-like maghemite particles for medical applications. At first, akaganeite rods with length of several hundred nm and width of ≈85 nm were prepared under hydrothermal conditions and were subsequently coated with mesoporous silica. Such coating enabled to maintain the shape of rods during the following steps that involved structural transformation of akaganeite to maghemite, i. e. γ-Fe_2O_3. Then the original protective coating was removed by alkaline leaching, bare maghemite rods were isolated, and their structure and ferrimagnetic order were characterized by X-ray diffraction, TEM inspection, Mössbauer spectroscopy and SQUID magnetometry. The magnetization of the bare maghemite rods, that were formed by elongated clusters of ≈10–20 nm crystallites, made 47.0 and 41.7 Am^2/kg in magnetic field of 3 T at 5 and 300 K, respectively. The hysteresis loops of both the bare and coated products at 300 K and ZFC/FC studies showed that the maghemite particles were largely blocked at room temperature in spite of the small size of crystallites. Finally, the particles were equipped with standard silica coating for biological studies. An evaluation of cytotoxicity of this silica-coated product was performed on two cell lines, namely A549 and MCF-7. The viability of cells incubated with particles at the concentration of 0.10, 0.21 and 0.42 mmol(Fe)/L was determined after 24 h and 48 h of incubation, and the values normalized to the viability of negative control were generally higher than 95 %. Moreover, the real-time monitoring of cell adhesion, proliferation, and cytotoxicity by an xCELLigence system during 72 h of the incubation with particles revealed only some decrease of the cell index for the MCF-7 cells at the high concentration.

1. Introduction

The remarkable diversity of iron oxide family, including not only iron oxides, but also iron hydroxides and oxyhydroxides, is manifested above all by various crystal structures and their magnetic properties, while such diversity is further enhanced on nanoscale level. Thus the stoichiometric iron(III) oxide of the simple formula Fe_2O_3 provides four different structural polymorphs, whose magnetic behaviours differ dramatically from the antiferromagnetic hematite (α-Fe_2O_3) and β-Fe_2O_3 systems, over the superparamagnetic maghemite (γ-Fe_2O_3) nanoparticles, to the nanocrystalline ε-Fe_2O_3 phase with giant coercivity. In addition, an entirely new polymorph ζ-Fe_2O_3 has been recently prepared by a high-pressure-induced transformation of ultrafine β-Fe_2O_3 particles [1].

Magnetic nanoparticles of spinel-type maghemite (iron(III) oxide) and magnetite (iron(II,III) oxide) are successfully employed for example in certain diagnostic methods based on MRI or as tracers for MPI, and plethora of new applications, including nanomedicine, catalysis, remediation, data storage, etc., are in progress. In the medical applications, the main concerns are in low toxicity or even biocompatibility and in the optimum size, which determines magnetic properties of the particles and influences their behaviour in biological systems, above all the fate after the administration into blood vessels. The use of magnetic particles as contrast agents for MRI and the most popular nanomedical concepts, e.g. magnetic targeting and magnetically triggered drug delivery, assume intravenous administration of particles that should be small enough that they can be disseminated in body through the blood circulation and can be eventually removed by normal physiological pathways. To meet such requirements, the maximum size of the particles should not exceed ≈75 nm. It can be noted, however, that for specific medical applications, much larger particles might suit better. Long time ago, iron-based microspheres of size 1–3 μm were used for the treatment of artery aneurysma, in which the magnetic particles were injected upstream and captured by permanent magnets to block the blood to enter the aneurismal opening before an occluding tissue was formed [2].

Very recently, the injectable formulation “Fibermag”, consisting of μm-size magnetic particles in biocompatible, fiber-forming polymers, was proposed for curing of a spinal cord injury [3]. The essence of this method is in formation of extended chains of these particles in response to externally applied magnetic field. This results in an alignment of the polymer fibers, making thus artificial scaffolds for axonal growth in the direction of the original nerve. At the present stage, the method was tested with using of spherical particles only. Nonetheless, in future search for higher efficiency, prolate or rod-like shapes may be prospective and fabrication of such magnetic cores with size of few μm deserves an attention.

Focusing on magnetic nanoparticles of highly anisotropic shapes, a method in which iron oxide systems are obtained by transformation of akaganeite precursors is especially promising. From the chemical point of view, the synthesis of akaganeite particles allows for excellent control of shape; for example nanorods [4], micrometer-sized rods [5] and well-defined crystal twins [6] can be achieved. Under suitable conditions, akaganeite crystallites can be also subjected to structural transformations, e.g. into magnetite/maghemite [7-9], hematite [10] or even ε-Fe_2O_3 [11], as well as to direct anion exchange to prepare β-FeO(OH) [7]. According to the previous studies, the conversion of akaganeite to an iron oxide of the spinel or spinel-like structure seems to be facile. These studies considered the resulting product to be magnetite, assuming that the application of reductive conditions (the use of hydrazine, the polyol method) leads to partial reduction of ferric ions [7, 8, 12]. However, no conclusive data on the actual oxidation state of iron, like Mössbauer

spectroscopy, have been reported for such products. The reduction of ferric ions by hydrazine, used in the traditional works [8, 12], is expectable, but the actual oxidation state of a product obtained under the conditions of the polyol method [7] desires more attention.

In the present study, hydrothermally synthesized akaganeite rods are used as a precursor for the preparation of magnetic rods of a nano-to-micro size, suitable for the aforementioned applications. The multistep procedure, involving protective coating with mesoporous silica, structural transformation under solvothermal conditions of the polyol method and additional thermal treatment, is applied to achieve the desired product with reasonable magnetization. The XRD and TEM are employed to analyse its phase composition and morphology, whereas the actual oxidation state of iron is determined by Mössbauer spectroscopy. The results confirm the maghemite nature of the transformed rods. Further, the rods of several hundred nm length and ≈85 nm average diameter are coated with silica shell of ≈15 nm thickness in order to be applicable for the biological studies. Magnetic properties relevant for the application are investigated by SQUID magnetometry and basic evaluation of cytotoxicity is performed on two cell lines.

2. Experimental details

2.1. Synthesis of akaganeite precursor

Mixture of 0.5 mL of oleic acid and 20 mL of water was prepared directly in a 50 mL Teflon insert of a Berghof DAB-2 autoclave by applying ultrasound agitation for 10 min. Then 10 mmol of urea and 3.75 mmol of $FeCl_3$ dissolved in 5 mL of water were added under the ultrasound agitation. The mixture was sealed in the autoclave and was heated to 90 °C for 10 h while magnetic stirring was applied. The product was thoroughly washed in several steps by using acetone, ethanol, water alkalized with ammonia and pure water, and was dried at 105 °C. The synthesis yielded 230 mg of the product.

2.2. Preparation of maghemite rods via an intermediate coated with mesoporous silica

At first, 200 mg of akaganeite precursor was dispersed in ice-cold 1 M nitric acid in an ultrasound bath for 15 min. After separation of the particles by centrifugation, similar treatment with ice-cold 0.1 M citric acid was applied. The particles were washed with water and were redispersed in 10 mL of water alkalized with few drops of ammonia by means of an ultrasound probe. The stable suspension was transferred into a solution of 0.8 g of cetyltrimethylammonium bromide (CTAB) in 300 mL of ethanol, 70 mL of water and 20 mL of ammonia. The suspension was stirred both mechanically and by ultrasound, and 610 µL of tetraethoxysilane (TEOS) was added. The next day, the product was separated by centrifugation and was washed thoroughly with ethanol. The residual CTAB present in the mesoporous coating was removed by ligand exchange procedure according to [13]. Specifically, the raw coated product was refluxed in 250 mL of an ethanol solution of 2.5 g of NH_4NO_3, and the coated particles were thoroughly washed with ethanol and water.

The particles after the ligand exchange were dispersed in a solution of 200 mg of sodium acetate in 40 mL of ethylene glycol. And the mixture was treated under autogenous pressure at 240 °C for 48 h in a Teflon insert of a Berghof DAB-2 autoclave. The particles were separated by centrifugation, washed with ethanol and water and dried in vacuo. Then, the material was subjected to heating under argon atmosphere in three steps at 500 °C, 600 °C and 700 °C for 4 h at each one. Finally, alkaline leaching of the original silica coating was carried out by heating the sample in 4 M NaOH at

80 °C in two cycles. The product was obtained by thorough washing with water and was dried in vacuo at 40 °C.

2.3. Preparation of silica-coated maghemite rods

The amount of 40 mg of maghemite rods was treated with ice-cold 1 M nitric acid and ice-cold 0.1 M citric acid, and a stable aqueous suspension was prepared just as in the case of coating the akaganeite precursor with mesoporous silica. The citrate-stabilized rods were encapsulated into silica in the mixture of 160 mL of ethanol, 40 mL of water and 10 mL of ammonia by adding 260 µL of TEOS. The mixture was mechanically stirred and tempered to 57 °C for 4 h. The coated particles were separated by centrifugation and were washed thoroughly by ethanol and water. Then, mild size fractionation was carried out by differential centrifugation at 29 rcf for 10 min. The corresponding supernatant was collected as the final product and was concentrated to 10 mL of water.

2.4. Characterizations

X-ray powder diffraction (XRD) was used to analyse the phase composition, crystal structure, and mean size of crystallites. The XRD patterns were obtained with CuKα radiation on a Bruker D8 diffractometer and were analysed by means of the Rietveld method in the program FULLPROF. The Thompson-Cox-Hastings pseudo-Voigt profile was applied to separate the strain and size contributions. The instrumental profile was determined on the basis of a strain-free tungsten powder with the crystallite size of 9.4 µm.

The chemical composition of the akaganeite precursor, i.e. the ratio of Fe and Cl, was determined by X-ray fluorescence spectroscopy (XRF).

The actual oxidation state of iron in bare maghemite rods was studied by ^{57}Fe Mössbauer spectroscopy. The measurements were carried out in transmission arrangement with a ^{57}Co/Rh source at room temperature and at the temperature of 4.2 K in a JANIS cryostat. The in-field spectra at 4.2 K were acquired in the external magnetic field of B_{ext} = 6 T applied perpendicular to the γ-ray direction. Calibration of velocities and isomer shifts was based on α-Fe at 296 K. The spectra were analysed by using CONFIT software.

The size and morphology of both bare and coated samples were studied by transmission electron microscopy (TEM) on a Philips CM 120 instrument. Image analysis of TEM micrographs of silica-coated maghemite rods was carried out by means of the ImageJ program to evaluate the distribution of length and width of their maghemite rod-like cores.

SQUID magnetometry was performed on well-compacted powder samples by employing a Quantum Design MPMS XL. The magnetization curves were measured up to the fields of 3183 kA/m at temperatures of 5 and 300 K. The ZFC-FC (zero-field-cooled and field-cooled) measurements were carried out in magnetic field of H = 1.59 kA/m. SQUID magnetometry was also used to determine the concentration of maghemite phase in the aqueous suspension of coated rods as follows. At first, an aliquot of the suspension was concentrated in an Eppedorf tube by exhaustive centrifugation. The residue was quantitatively transferred onto a small piece of Teflon tape while being dispersed in ≈100 µL of water. The droplet was slowly evaporated and dried at 105 °C. Then its magnetic moment

was measured at 5 K in magnetic field of 796 kA/m and was compared with the magnetization of bare maghemite rods.

2.5. Evaluation of cytotoxicity

2.5.1. Cell cultures

The human lung carcinoma cell line A549 and human breast adenocarcinoma cell line MCF-7 were obtained from the European Collection of Authenticated Cell Cultures (ECACC). A549 cells were cultured in Minimum Essential Medium Eagle with L-glutamine and sodium bicarbonate (Sigma-Aldrich) in the presence of 10 wt% foetal calf serum, 1 mmol/L pyruvate, 10 mmol/L HEPES, 50 µg/mL penicillin, and 50 µg/mL streptomycin (all supplements from Life Technologies). MCF-7 cells were maintained in Minimum Essential Medium Eagle with L-glutamine and sodium bicarbonate (Sigma-Aldrich) supplemented with 10 wt% foetal calf serum, 1 µg/mL insulin, 50 µg/mL penicillin and 50 µg/mL streptomycin (all reagents from Life Technologies). Both the cell lines were maintained and grown at 37 °C, 95 % humidity, 5 % CO_2. And for both the A549 and MCF-7, cells in the maximum range of 20 passages and in an exponential growth phase were used for this study.

2.5.2. Real-time monitoring of cells by xCELLigence system

The RTCA SP xCELLigence system (Roche and ACEA Biosciences) was used to monitor cell adhesion, proliferation, and cytotoxicity of silica-coated maghemite rods for both the A549 and MCF-7 cell lines. The system had been tested by a Resistor Plate before the RTCA Single Plate station was placed inside the incubator at 37 °C with 5 % CO_2. First, the optimal seeding concentration for experiments with both types of cells was determined. Background measurements were taken by adding 100 µL of an appropriate medium to wells of an E-Plate 96. Then, cell suspension (90 µL) was added to each well at the density of 7,000 and 20,000 cells per well for A549 and MCF-7, respectively. The cells were monitored every 30 minutes by the xCELLigence system. Approximately 24 h later, when the cells were in the log growth phase, they were exposed to 10 µL of tested particles diluted with sterile deionized water for cell cultures (Lonza) to obtain final concentrations of 0.10, 0.21 and 0.42 mmol(Fe)/L in the E-Plate wells. Negative controls received sterile deionized water for cell cultures (Lonza), whereas cells treated with 5 % DMSO were used as positive controls. All experiments were carried out in tetraplicates and run for 72 h after the treatment. Data analysis was performed by using the xCELLigence 1.2.1 software.

2.5.3. Proliferation and viability

A549 and MCF-7 cells were seeded at a concentration 150,000 cells/25 cm^2 Falcon flask and treated with silica-coated maghemite rods at the final concentrations of 0.10, 0.21 and 0.42 mmol(Fe)/L in the medium. Further, cells treated with 1 µmol/L doxorubicin (Sigma-Aldrich) were used as positive control. Cell proliferation and viability of A549 and MCF-7 cells were determined 24 and 48 hours following treatment. The cells were detached with 0.05 % trypsin-EDTA (Life Technologies) applied for 8 minutes. The detached cells were pooled with floating cells present in medium. The cell

membrane integrity was determined by using the trypan blue exclusion technique. For this purpose, 50 µL of a cell suspension was mixed with 50 µL of 0.4% Trypan blue (Sigma-Aldrich). Cell counts were evaluated by using a Bürker chamber and a light microscope Nikon Eclipse E200. All experiments were carried out in doublets.

3. Results and discussion

3.3. Synthesis, structure and morphology of particles

According to XRD patterns depicted in Fig. 1, the akaganeite precursor was prepared as a single-phase product whose structure can be described by the *I*2/m space group, see refs. [14-16] for more details on the akaganeite structure. The lattice parameters of the monoclinic cell were refined to *a* = 10.5228(20) Å, *b* = 3.0242(3) Å, *c* = 10.4670 (10) Å and *β*= 89.62 (1)°.

The pattern of the bare final product prepared from the akaganeite precursor and denoted here as maghemite rods (see below the Mössbauer spectroscopy) is more or less consistent with both the maghemite and magnetite structures, and the given XRD data do not allow to distinguish these phases reliably. However, the minor diffraction peak at $2\theta \approx 15°$ indicates a deviation from the $Fd\bar{3}m$ space group, which is the symmetry of magnetite and maghemite with random distribution of vacancies. Thus, this minor peak supports the presence of maghemite with at least some ordering of vacancies, namely either the cubic phase with partial ordering of vacancies and symmetry described by the enantiomorphous pair $P4_132/P4_332$ or the tetragonal phase with full vacancy ordering and symmetry of the $P4_12_12/\ P4_32_12$ pair [17]. Considering the results of Mössbauer spectroscopy, the refinement of the tetragonal structure was carried out and provided lattice parameters *a* = 8.327(5) Å and *c* = 25.129(28) Å. Compared to the akaganeite sample, the pattern of maghemite rods was affected by much larger line broadening, which resulted from a small size of crystallites that delimited the XRD coherence length. The so-called mean size of crystallites, i.e. the size of coherent diffraction domains within the polycrystalline rods, was evaluated to ≈10–20 nm.

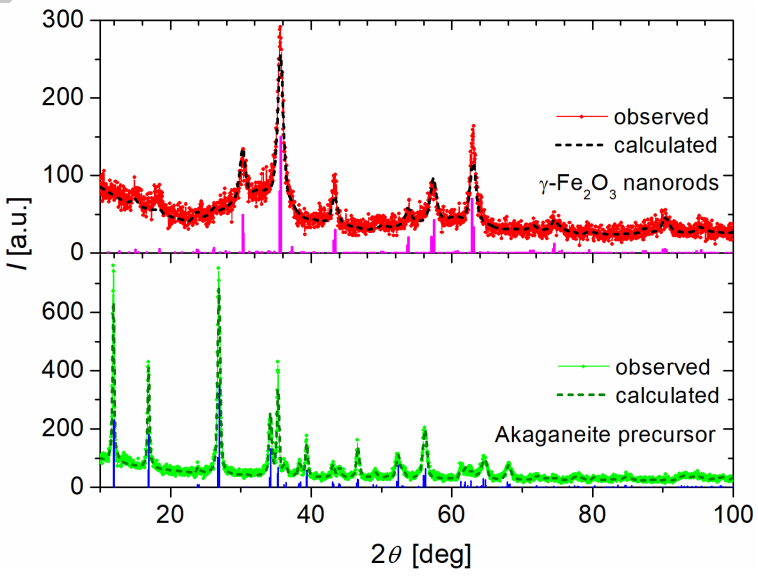

Fig. 1. XRD patterns of the akaganeite precursor and the final product (maghemite rods). The observed data are supplemented by calculated patterns. The blue vertical lines indicate diffractions of the monoclinic akaganeite structure, whereas the vertical magenta lines show diffractions of the tetragonal maghemite phase.

In order to resolve the nature of the final product, the ^{57}Fe Mössbauer spectroscopy in zero external magnetic field and at B_{ext} = 6 T was performed. The spectra measured at liquid helium temperature (see Fig. 2) showed that no verifiable amount of Fe^{2+} ions is present, and thus the product is not the Fe(II)/Fe(III) magnetite but can be unambiguously classified as Fe(III) maghemite. The measurements at low temperature also evidenced ferrimagnetic ordering of the structure. Importantly, the application of the external magnetic field $\boldsymbol{B}_{ext}$ in addition to the magnetic hyperfine field $\boldsymbol{B}_{hf}$ at the ^{57}Fe nuclei results in the decrease of the effective magnetic field of the octahedral sites according to $\boldsymbol{B}_{eff} = \boldsymbol{B}_{hf} + \boldsymbol{B}_{ext}$ and in the increase of $\boldsymbol{B}_{eff}$ of the tetrahedral sites due to the opposite orientation of magnetic moments. This fact simplifies the analysis of multiple components present in the spectra of the studied sample.

The room-temperature spectrum evidenced significant broadening of spectral lines and suggested presence of small nanoparticles that were partly in the superparamagnetic regime (roughly 27 % of the sample was superparamagnetic at the time scale of Mössbauer spectroscopy, i.e. ~10^{-7} s). The component affected by superparamagnetic relaxation (see the different components in the upper panel of Fig. 2) involves the contributions of both octahedral and tetrahedral sites, and is characteristic by very broad distribution of magnetic hyperfine field and by quadrupole splitting averaged to zero. No paramagnetic doublet was observed in the spectrum.

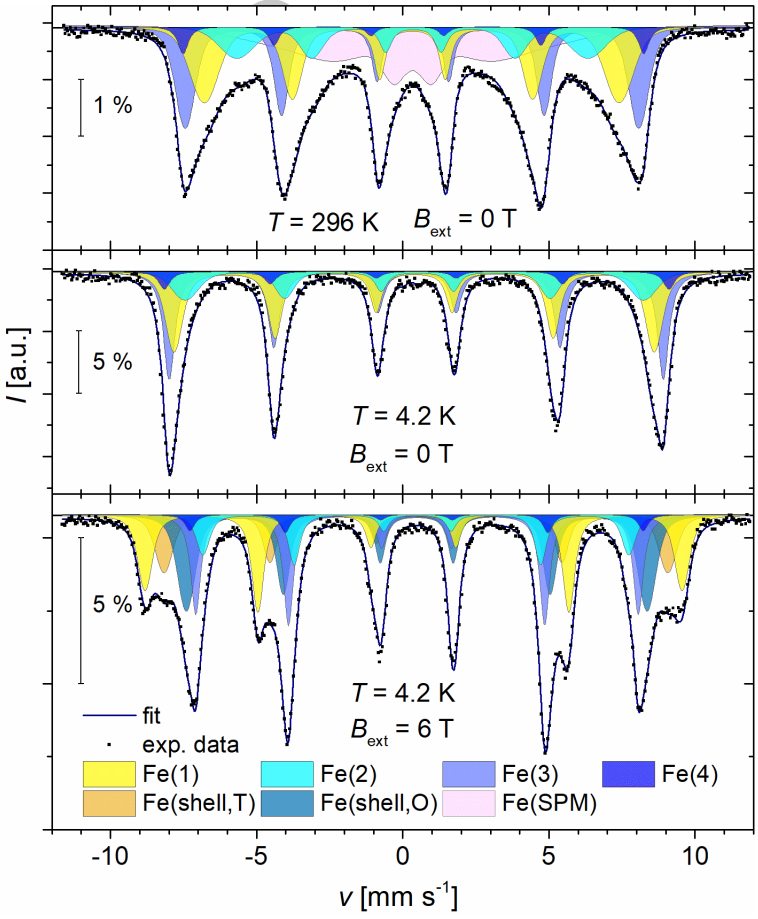

Fig. 2. Mössbauer spectra of maghemite rods at room temperature and at 4.2 K in zero field and in an external magnetic field of B_{ext} = 6 T. The vertical scale denotes the effect of the measured spectra. Tetrahedral sites include Fe(1) and Fe(shell,T), whereas Fe(2), Fe(3), Fe(4) and Fe(shell,O) are octahedral positions. At room temperature, a component affected by superparamagnetic (SPM) relaxation is present. For the in-field spectrum, the shell components, Fe(shell,T) and Fe(shell,O), were fitted separately from the other components.

The spectra measured at 4.2 K were analysed by using three different maghemite models with various degrees of vacancy ordering (for the structures considered in the fitting procedure see Table 1). The ratios of the constituent sextets related to individual iron sites were fixed during the fitting procedure, the same Lamb-Mössbauer factors were considered for all sites. The best fit was obtained for the simplified model of the maghemite $P4_32_12$ structure based on an average subcell, as suggested by C. Greaves [18], instead of the tripled tetragonal cell. This model includes only four non-equivalent iron sites compared to nine components of the tripled cell, whose fitting was not considered reasonable due to the high number of refined parameters. The spectra fitted by the simplified model along with the components of the fit are shown in fig. 2, the obtained hyperfine parameters are summarised in table 2. The isomer shifts of the tetrahedral sites, ∼0.37, and of octahedral sites, ∼0.47, are in good agreement with, e.g. [19], and no sextet with isomer shift higher than 1 related to Fe^{2+} ions was observed.

For the interpretation of the in-field spectrum of maghemite rods, the core-shell model [20, 21] was employed. Specifically, collinear ordering of magnetic moments in the four Fe(1)–Fe(4) sextets in the core of nanocrystallites and disorder of magnetic moments in their shell were presumed. Therefore, the analysis included two additional components specific to the shell, one component for tetrahedral sites, another one for octahedral sites. Generally, the outer, middle and inner line intensities of a component sextet are related by the ratio of 3 : $(4\sin^2\vartheta)/(1+\cos^2\vartheta)$: 1, where ϑ is the angle between the γ-ray direction and the nuclear magnetic moment [22]. The Fe magnetic moments in the core were almost fully reoriented to the direction of the external magnetic field, which can be deduced from the ratio of intensities of the individual spectral lines in the core sextets 3 : 3.33 : 1 compared to the ideal full reorientation that yields the ratio of 3 : 4 : 1 for an external magnetic field applied perpendicularly to the γ-ray direction. Further, the effective magnetic field of the core components increased (decreased) almost by the applied 6 T at the tetrahedral (octahedral) iron sites. In contrast, the ratio of line intensities of the shell components approached 3 : 2 : 1, which suggests a random orientation of magnetic moments in the shell. This magnetic disorder is also consistent with the paraprocess in high fields observed by magnetic measurements (see hysteresis loops in fig. 5). Nevertheless, partial reorientation of the shell moments in the external magnetic field was demonstrated by slight increase/decrease of the effective field at corresponding sites.

Table 1. Overview of the space groups that describe maghemite phases with different degree of vacancy ordering and related Fe sites according to ref. [17]: *O* denotes site occupancy and *A* is the fraction of the given site as seen in Mössbauer spectra if equal Lamb-Mössbauer factors are considered for all Fe sites.

Space group	Fe site	Wyckoff position	Site symmetry	*O*(Fe)	*O*(vacancy)	*A*
$Fd\bar{3}m$	Fe(T)	8a	*-43m*	1	0	0.375
	Fe(O)	16d	*.-3m*	5/6	1/6	0.625
$P4_32$	Fe(1)	8c	*.3.*	1	0	0.375
	Fe(2)	4b	*.32*	1/3	2/3	0.0625
	Fe(3)	12d	*.3.*	1	0	0.5625

$P4_32_12$ (simplified model [18])	Fe(1)	8b	*1*	1	0	0.375
	Fe(2)	4a	*..2*	1	0	0.1875
	Fe(3)	8b	*1*	1	0	0.375
	Fe(4)	4a	*..2*	1/3	2/3	0.0625

Table 2. Hyperfine parameters obtained from the Mössbauer spectra of maghemite rods. The structural model based on an average subcell in the $P4_32_12$ representation according to ref. [18] was employed. *IS* denotes isomer shift, *QS* is quadrupole splitting, B_{eff} is the effective magnetic field at a nucleus given by $\boldsymbol{B}_{eff} = \boldsymbol{B}_{hf} + \boldsymbol{B}_{ext}$ and *A* denotes the area fraction of the respective component. Fixed parameters are marked by an asterisk.

Conditions	Component	*IS* [mm s^{-1}]	*QS* [mm s^{-1}]	B_{eff} [T]	*A*
T = 296 K B_{ext} = 0 T	Fe(1)	0.32(2)	-0.03(3)	44.1(3)	0.274*
	Fe(2)	0.35(3)	-0.04(4)	37.3(4)	0.137*
	Fe(3)	0.33(2)	0.03(3)	48.2(2)	0.274*
	Fe(4)	0.26(3)	0.21(4)	49.0(3)	0.046*
	Fe(SPM)	0.34(6)	-	-	0.27(1)
T = 4.2 K B_{ext} = 0 T	Fe(1)	0.39(2)	0.00(3)	51.0(3)	0.375*
	Fe(2)	0.45(3)	-0.10(5)	48.7(4)	0.1875*
	Fe(3)	0.47(2)	-0.04(3)	52.7(2)	0.375*
	Fe(4)	0.37(2)	0.21(6)	53.6(4)	0.0625*
T = 4.2 K B_{ext} = 6 T	Fe(1)	0.37(2)	0.01(3)	57.0(3)	0.217(5)
	Fe(2)	0.48(3)	-0.05(3)	45.4(3)	0.109(3)
	Fe(3)	0.49(2)	0.02(3)	47.1(2)	0.217(5)
	Fe(4)	0.37(5)	-0.04(6)	47.3(5)	0.036(1)
	Fe(shell,T)	0.45(3)	0.00*	53.5(3)	0.158(5)
	Fe(shell,O)	0.48(3)	0.00*	48.9(3)	0.26(2)

The actual chemical composition of the akaganeite precursor was refined to $FeO_{0.89}(OH)_{1.11}Cl_{0.11}$ based on the Fe : Cl ratio determined accurately by XRF analysis. The final product obtained by the hydrothermal treatment and subsequent heating was not analysed by XRF since the structural transformation of akaganeite to maghemite/magnetite structure was necessarily accompanied by the loss of all chloride anions.

Representative TEM images of the akaganeite precursor, bare maghemite rods and the silica-coated product are shown in Fig. 3. The akaganeite precursor is formed by rod-like particles, whose length extends up to several hundred nm and whose average width is around ≈85 nm. In spite of the structural transformation under solvothermal conditions and subsequent heating to 700 °C, the same overall shape of particles is also observed for the final maghemite product, which was enabled by the encapsulation of akaganeite rods into low-density mesoporous silica. Such protective coating helped to preserve the original shape and prevented individual particles to grow together (see, e.g. the application of silica coating before thermal treatment of molten-salt-synthesized manganite nanoparticles that was used to enhance their magnetic properties [23]), while open mesopores (typical diameter of ≈3 nm, see the sample prepared by CTAB-assisted procedure in [24]) in the coating made the transformation of akaganeite to the spinel structure possible. However, TEM inspection of the rod-like maghemite particles revealed more complex morphology. The patchy morphology reflects their polycrystalline character that was expected based on the small size of crystallites determined by XRD.

To provide colloidal stability in an aqueous suspension and to avoid undesired interactions of the particles with biological systems, such as gradual biodegradation and deterioration of magnetic properties, maghemite rods were coated by standard amorphous silica. The resulting product, further employed in biological studies, was characterized by a typical smooth silica shell with the thickness of ≈15 nm. The suppressed aggregation of the coated particles also enabled to evaluate the size distribution of the rods based on TEM data, see Fig. 4.

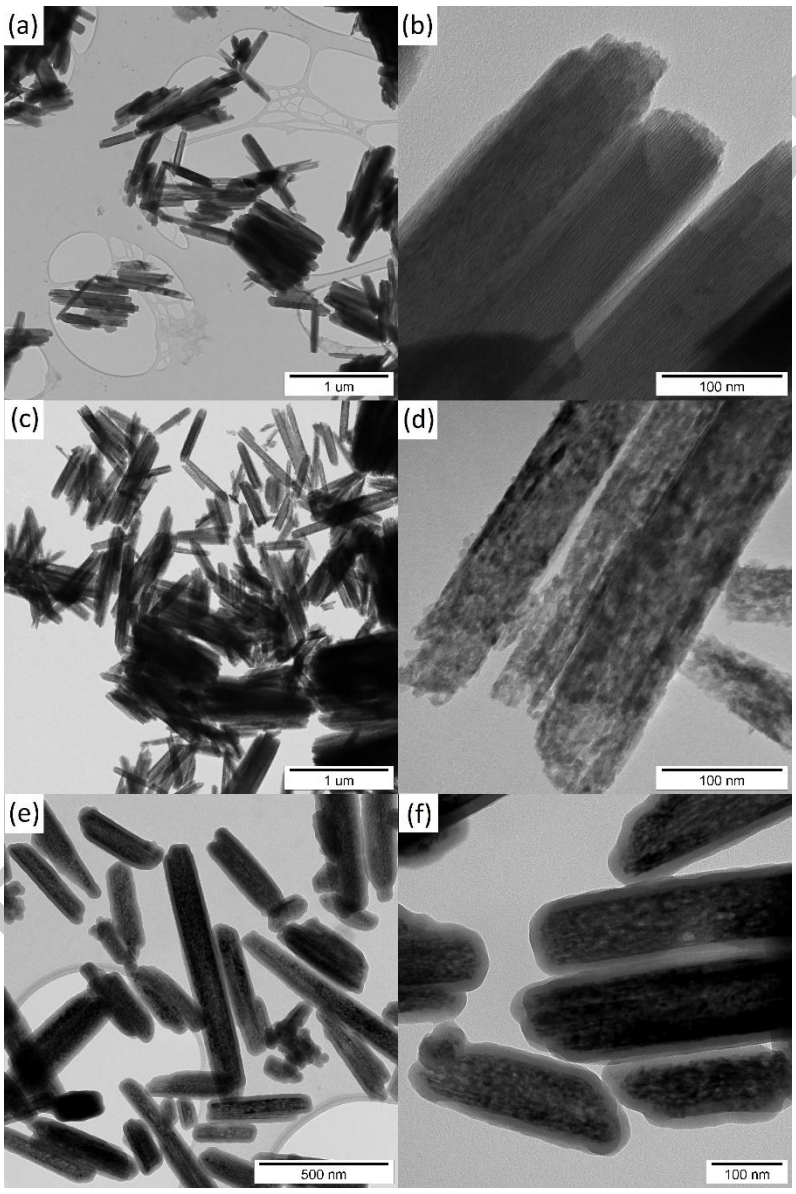

Fig. 3. Transmission electron micrographs: (a, b) akaganeite precursor, (c, d) maghemite rods, and (e, f) silica-coated maghemite sample.

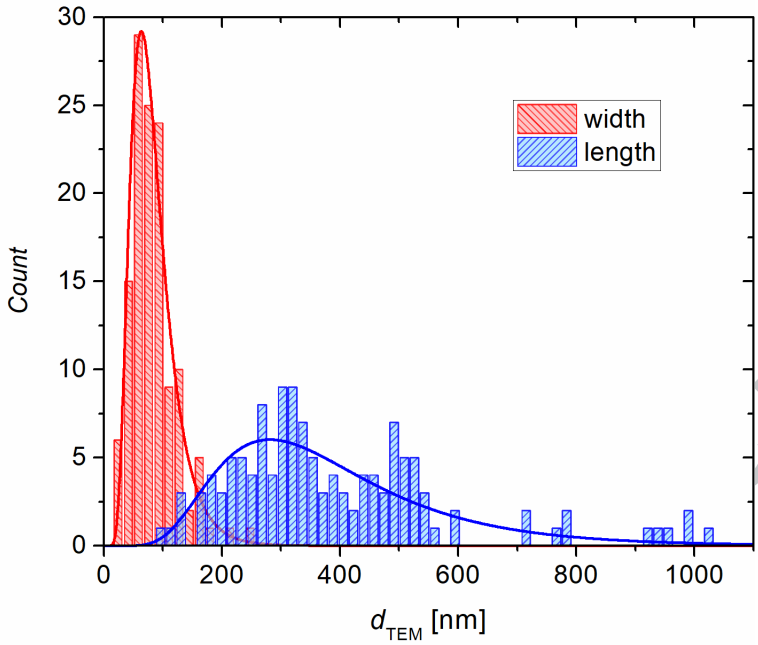

Fig. 4. Size distribution of maghemite rods in the coated product. Separate histograms are shown for the length and width of the rod-like cores.

3.4. Magnetic properties

The low- and room-temperature hysteresis loops for the bare and silica-coated maghemite rods and the akaganeite precursor are depicted in Fig. 5a,b. As regards the akaganeite precursor, its linear anhysteretic response to external magnetic field at 300 K is given by its paramagnetic nature. At 5 K the precursor is in antiferromagnetic state, characterized by a linear paraprocess. There is in addition only hardly observable ferromagnetic-like contribution of M = 0.05 Am^2/kg and H_c = 35 kA/m. This contribution could be probably ascribed to uncompensated spins of akaganeite particles [4, 25] rather than to a minor impurity. When related to the akaganeite amount, it gives the magnetization of only $8.4 \cdot 10^{-4}$ μ_B per formula unit of $FeO_{0.89}(OH)_{1.11}Cl_{0.11}$, which can be compared with the uncompensated magnetization of $3.5 \cdot 10^{-4}$ μ_B per Fe of bulk akaganeite that arises from minor spin canting [4].

The specific magnetization of bare maghemite rods in Fig. 5a reaches 47.0 Am^2/kg at 5 K in magnetic field of 3 T and decreases only to 41.7 Am^2/kg at 300 K. The magnetization of spontaneous ordering at 5 K, evaluated by an extrapolation to zero field, is 42.9 Am^2/kg, which gives magnetic moment of 1.23 μ_B per formula unit of Fe_2O_3. The bare rods are characterized by coercive field H_c = 29 kA/m at 5 K and exhibit some hysteresis also at 300 K with H_c = 6.2 kA/m. The specific magnetization of the coated product is lower since the diamagnetic silica diluted the ferrimagnetic maghemite phase, and its value of 21.2 Am^2/kg at 5 K in the field of 3 T allows us to estimate the maghemite weight content in the coated sample to 45 %. The hysteresis loops of the coated product shows the same coercive field as the bare rods.

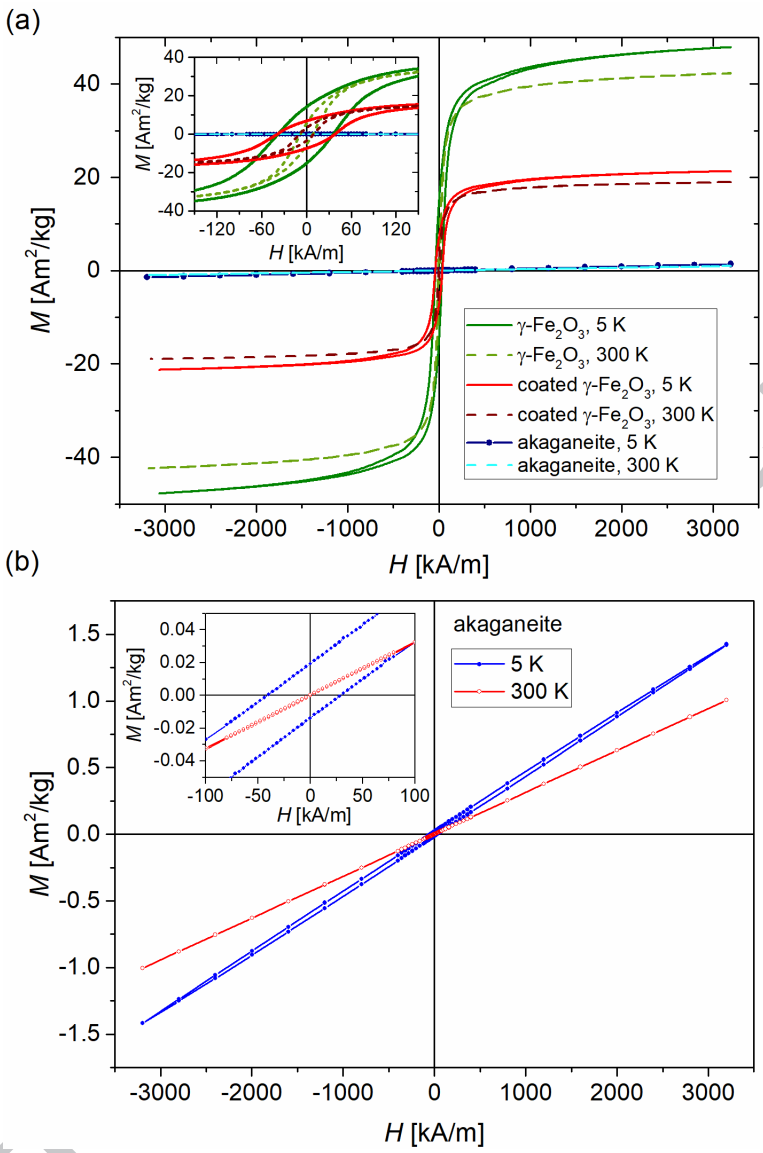

Fig. 5. Hysteresis loops of bare maghemite rods and silica-coated product at temperatures of 5 K and 300 K (a). Enlarged magnetization data for akaganeite at 5 K and 300 K (b).

The DC susceptibility measurements in ZFC/FC regimes are displayed in Fig. 6. The study of both bare and coated products confirmed that maghemite nanocrystallites within the polycrystalline rods, albeit as small as ≈10–20 nm, remain in blocked state at 300 K and the irreversibility temperature, i.e. the bifurcation point of the ZFC/FC susceptibility curves occurs at much higher temperatures. This observation, consistent with the room-temperature coercive field of 6.2 kA/m, suggests that clustered maghemite crystallites do not behave independently but strong interparticle interactions are present.

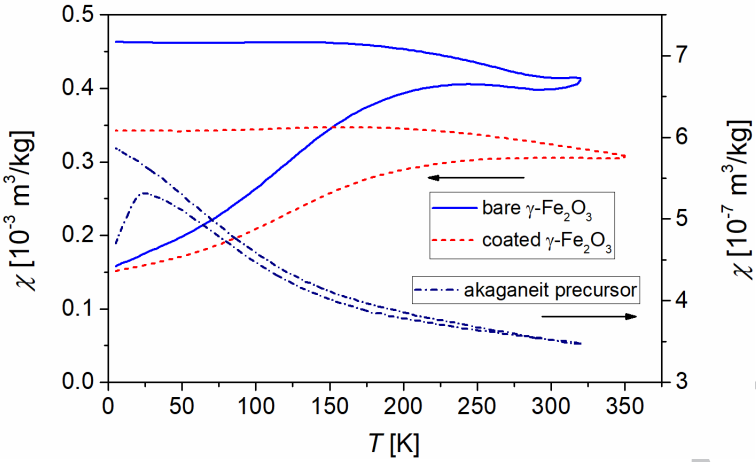

Fig. 6. Temperature dependence of magnetic susceptibility measured in ZFC and FC regimes in magnetic field of 1.59 kA/m.

3.5. Cytotoxicity of silica-coated maghemite rods

The quantification of viability and growth of cells treated with silica-coated maghemite rods is summarized in Fig. 7 and Table 3 for both cell lines A549 and MCF-7. Neither the cell viabilities nor the numbers of harvested cells indicated any toxic effect of coated particles up to the concentration of 0.42 mmol(Fe)/L. Generally, the viabilities of treated cells normalized to the viability of respective negative controls were generally higher than 95 % for both types of cells and for the evaluation of viability both after 24 and 48 h. In contrast, the incubation of cells with doxorubicin, a standard chemotherapeutic drug administered intravenously, under the same conditions and at the concentration as low as 1 µmol/L led to a dramatic decrease in cell viability. The numbers of cells harvested after 24 h and 48 h incubation were either not significantly different from the negative control or exhibited only small and random variation, which was not correlated with the concentration of particles.

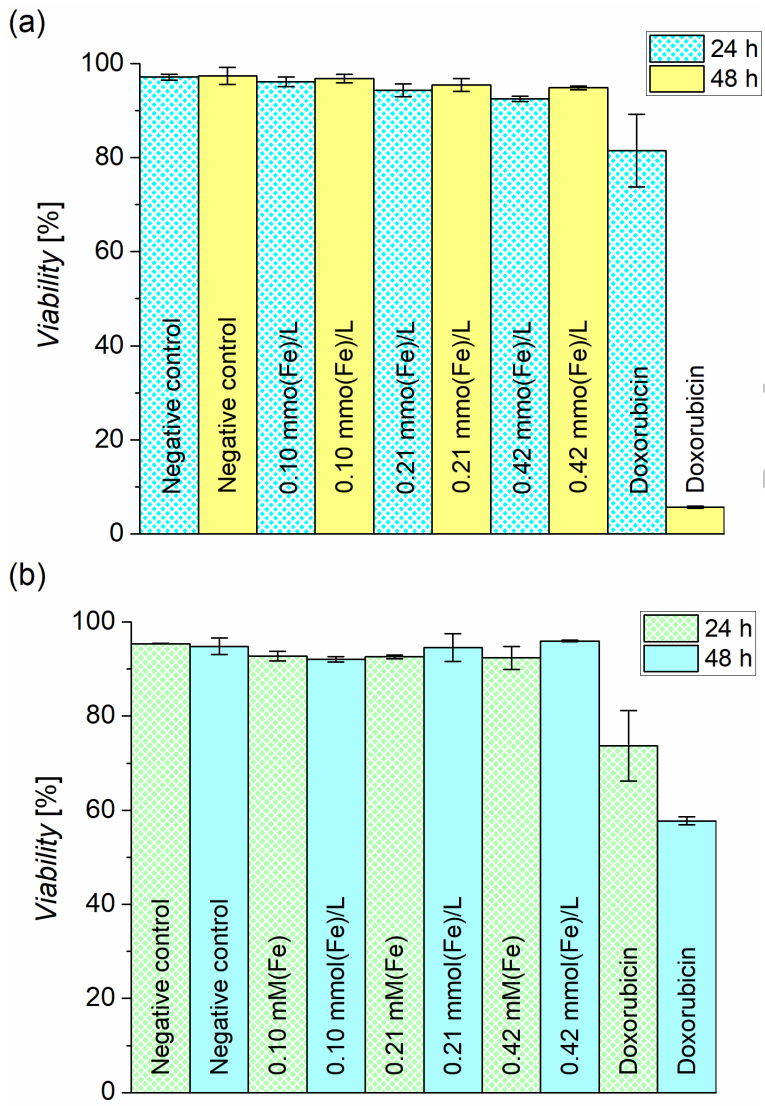

Fig. 7. Viability of (a) A549 and (b) MCF-7 cells incubated with silica-coated maghemite rods at different concentrations. The viability was determined by the trypan blue exclusion test 24 h and 48 h following the treatment. Cells treated with doxorubicin at the concentration of 1 µmol/L and cells treated with sterile deionized water were used as the positive and negative controls, respectively. Results are shown as mean values ± standard deviations of two independent experiments.

Table 3. Growth of A549 and MCF-7 cells incubated with silica-coated maghemite rods at different concentrations and evaluated 24 and 48 hours after treatment. The values give the mean ratio of the number of cells harvested and the number of cells seeded.

	A549 cells		MCF-7 cells	
	24 h	48 h	24 h	48 h
Negative control	3.27	8.42	2.13	4.00
0.10 mmol(Fe)/L	3.11	6.87	2.13	3.18
0.21 mmol(Fe)/L	3.24	8.04	2.02	3.73
0.42 mmol(Fe)/L	3.04	8.64	2.40	4.04
Doxorubicin - 1 µmol/L	1.20	0.044	1.00	0.49

To further study cytotoxic effects of silica-coated maghemite rods, the real-time monitoring of both types of cells incubated with particles at different concentrations was performed by the xCELLigence system. The normalized cell index (*CI*), reflecting the cell proliferation, adhesion and viability, is shown in Fig. 8. As regards the A549 cells, almost no effects of particles were observed up to the concentration of 0.42 mmol(Fe)/L, not even after 72 hours of the incubation. Interestingly, some decrease in the cell index with the increasing concentration of particles was found for the MCF-7 model. Specifically, at high concentration of 0.42 mmol(Fe)/L, the silica-coated rods negatively affected the proliferation.

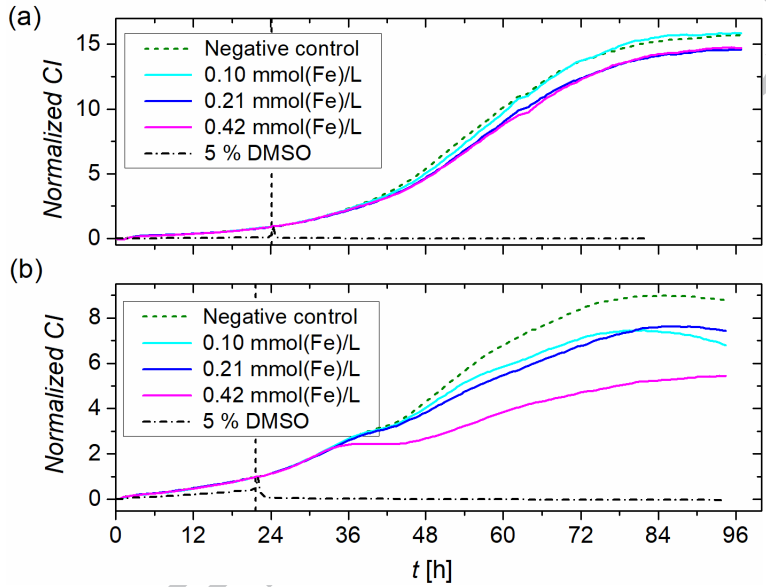

Fig. 8. Real-time monitoring of cell adhesion, proliferation and cytotoxicity by an xCELLigence system: (a) A549 cells and (b) MCF-7 cells treated with silica-coated maghemite rods at different concentrations. The negative control was treated with sterile deionized water for cell cultures, while 5 % DMSO was used as the positive control. The dashed vertical lines indicate the time of treatment with particles.

3. Conclusions

The akaganeite group comprises monoclinic phases (alternatively and mostly earlier considered to be tetragonal) of the general composition FeO(OH,Cl), including the oxide-hydroxide β-FeO(OH), that originate especially in chloride-rich environments. Their hollandite-related structure is formed by $Fe(O,OH)_6$ octahedra that share either edges or corners and create 4 × 4 Å large one-dimensional voids parallel to the *b* axis of the monoclinic representation. These channels contain variable amount of chloride anions that are coordinated via hydrogen bonds to hydroxyl groups of $Fe(O,OH)_6$ [26]. This structural arrangement is the reason for formation of rod-shape crystals or may lead, in nanoscopic case, to ellipsoidal single-crystal particles. For the present study, submicroscopic akaganeite rods (length of up to several hundred nm, width of ≈85 nm,) were employed for preparation of maghemite rods, intended for medical applications. The akaganeite-maghemite transformation was achieved under hydrothermal conditions and the crystallinity of the product was improved by subsequent thermal treatment, whereas the rod-shape character of maghemite was maintained by isolating akaganeite particles by mesoporous silica, which is characterized by low density and presence of open pores. Finally, this shell was removed leaving bare maghemite rods that were actually formed by elongated clusters of ≈10–20 nm crystallites. Their hysteresis loops

measured at 300 K and the ZFC/FC susceptibility curves showed that the rod-shaped particles were largely blocked at room temperature.

For biological studies, the maghemite rods were coated with a standard amorphous silica shell with the thickness of ≈15 nm to provide the particles with colloidal stability in aqueous environment and to isolate them from a biological system by a suitable coating. First, the hydrophilic surface of silica is biologically inert and enables facile covalent functionalization. Second, eukaryotic cells cannot carry out biodegradation of silica, and thus the leaching of iron ions from maghemite particles is permanently hindered by the stable and thick shell. This seems to be important for applications that demand long-term biostability of iron oxide particles and their magnetic properties, otherwise the gradual biodegradation of the particles would occur [27]. At the same time, adverse effects related to the release of iron ions from particles and their increased concentration are prevented. Actually, the studied silica-coated maghemite rods did not show any toxic effects during 24 and 48-hour incubation with two different cell lines, A549 and MCF-7, in the concentration range up to 0.42 mmol(Fe)/L. Moreover, the real-time monitoring of cell adhesion, proliferation and viability of both types of cells incubated with the particles as long as 72 h revealed only some decrease of the cell index for the MCF-7 line at the high concentration of 0.42 mmol(Fe)/L.

Acknowledgements

The study was financially supported by the Czech Science Foundation under the project 18-13323S. The physical part of the study was also supported by Operational Programme Research, Development and Education financed by European Structural and Investment Funds and the Czech Ministry of Education, Youth and Sports (Project No. SOLID21 - CZ.02.1.01/0.0/0.0/16_019/0000760). Finally, we would like to thank to our colleague Tomáš Kmječ for the kind help with the XRF analysis.

References

[1] J. Tuček, L. Machala, S. Ono, A. Namai, M. Yoshikiyo, K. Imoto, H. Tokoro, S. Ohkoshi, R. Zbořil, Zeta-Fe_2O_3 - A new stable polymorph in iron(III) oxide family, Scientific Reports, 5 (2015) 15091. 10.1038/srep15091.

[2] D.A. Roth, Occlusion of Intracranial Aneurysms by Ferromagnetic Thrombi, Journal of Applied Physics, 40 (1969) 1044-1045. 10.1063/1.1657525.

[3] J. Dapprich, R. Gilbert, K.P. Dresdner Jr., C. Johnson, Superparamagnetic particle scaffold for regenerating damaged neural tissue, United States Patent Application no. US 2018/0064951 A1.

[4] A. Urtizberea, F. Luis, A. Millán, E. Natividad, F. Palacio, E. Kampert, U. Zeitler, Thermoinduced magnetic moment in akaganéite nanoparticles, Physical Review B, 83 (2011) 214426. 10.1103/PhysRevB.83.214426.

[5] N. Hijnen, P.S. Clegg, Simple Synthesis of Versatile Akaganeite-Silica Core-Shell Rods, Chemistry of Materials, 24 (2012) 3449-3457. 10.1021/cm301772p.

[6] R.M. Cornell, Preparation and Properties of Si Substituted Akaganéite (β-FeOOH), Zeitschrift für Pflanzenernährung und Bodenkunde, 155 (1992) 449-453. doi:10.1002/jpln.19921550516.

[7] J. Choi, J. Cha, J.K. Lee, Synthesis of various magnetite nanoparticles through simple phase transformation and their shape-dependent magnetic properties, RSC Advances, 3 (2013) 8365-8371. 10.1039/c3ra40283e.

[8] M. Blesa, M. Mijalchik, M. Villegas, G. Rigotti, Transformation of akaganeite into magnetite in aqueous hydrazine suspensions, Reactivity of Solids, 2 (1986) 85-94. 10.1016/0168-7336(86)80066-3.

[9] S.A. Kahani, M. Jafari, A new method for preparation of magnetite from iron oxyhydroxide or iron oxide and ferrous salt in aqueous solution, Journal of Magnetism and Magnetic Materials, 321 (2009) 1951-1954. 10.1016/j.jmmm.2008.12.026.

[10] S. Goñi-Elizalde, M. E. Garcia-Clavel, I. Tejedor-Tejedor, Mechanism of Akaganeite-Hematite Transformation via Solution, Reactivity of Solids, 3 (1987) 139-154. 10.1016/0168-7336(87)80024-4.

[11] M. Tadic, I. Milosevic, S. Kralj, M. Mitric, D. Makovec, M.-L. Saboungi, L. Motte, Synthesis of Metastable Hard-Magnetic ε-Fe_2O_3 Nanoparticles from Silica-Coated Akaganeite Nanorods, Nanoscale, 9 (2017) 10579-10584. 10.1039/c7nr03639f.

[12] Z. Peng, M. Wu, Y. Xiong, J. Wang, Q. Chen, Synthesis of Magnetite Nanorods through Reduction of β-FeOOH, Chemistry Letters, 34 (2005) 636-637. 10.1246/cl.2005.636.

[13] N. Lang, A. Tuel, A fast and efficient ion-exchange procedure to remove surfactant molecules from MCM-41 materials, Chemistry of Materials, 16 (2004) 1961-1966. 10.1021/cm030633n.

[14] J.E. Post, V.F. Buchwald, Crystal structure refinement of Akaganeite, American Mineralogist, 76 (1991) 272-277.

[15] K. Ståhl, K. Nielsen, J. Jiang, B. Lebech, J.C. Hanson, P. Norby, J. van Lanschot, On the akaganéite crystal structure, phase transformations and possible role in post-excavational corrosion of iron artifacts, Corrosion Science, 45 (2003) 2563-2575. 10.1016/S0010-938X(03)00078-7.

[16] J.E. Post, P.J. Heaney, R.B. Von Dreele, J.C. Hanson, Neutron and temperature-resolved synchrotron X-ray powder diffraction study of akaganeite, American Mineralogist, 88 (2003) 782-788.

[17] K. Kelm, W. Mader, The Symmetry of Ordered Cubic γ-Fe_2O_3 Investigated by TEM, 2006 Zeitschrift für Naturforschung B, 61 (2006) 665-671. 10.1515/znb-2006-0605.

[18] C. Greaves, A powder neutron diffraction investigation of vacancy ordering and covalence in γ-Fe_2O_3, Journal of Solid State Chemistry, 49 (1983) 325-333. 10.1016/s0022-4596(83)80010-3.

[19] F. Menil, Systematic trends of the ^{57}Fe Mössbauer isomer shifts in (FeO_n) and (FeF_n) polyhedra. Evidence of a new correlation between the isomer shift and the inductive effect of the competing bond *T-X* (→ Fe) (where X is O or F and T any element with a formal positive charge), Journal of Physics and Chemistry of Solids, 46 (1985) 763-789. 10.1016/0022-3697(85)90001-0.

[20] J.M.D. Coey, Noncollinear Spin Arrangement in Ultrafine Ferrimagnetic Crystallites, Physical Review Letters, 27 (1971) 1140-1142. 10.1103/PhysRevLett.27.1140.

[21] T.J. Daou, J.-M. Greneche, S.-J. Lee, S. Lee, C. Lefevre, S. Bégin-Colin, G. Pourroy, Spin Canting of Maghemite Studied by NMR and In-Field Mössbauer Spectrometry, Journal of Physical Chemistry C, 114 (2010) 8794-8799. 10.1021/jp100726c.

[22] P. Gütlich, E. Bill, A.X. Trautwein, Mössbauer Spectroscopy and Transition Metal Chemistry: Fundamentals and Applications, Springer Berlin, Heidelberg (2010).

[23] M. Kačenka, O. Kaman, S. Kikerlová, B. Pavlů, Z. Jirák, D. Jirák, V. Herynek, J. Černý, F. Chaput, S. Laurent, I. Lukeš, Fluorescent magnetic nanoparticles for cell labeling: Flux synthesis of manganite

particles and novel functionalization of silica shell, Journal of Colloid and Interface Science, 447 (2015) 97-106. 10.1016/j.jcis.2015.01.071.

[24] J. Stergar, Z. Jirák, P. Veverka, L. Kubíčková, J. Kuličková, K. Knížek, F. Porcher, J. Kohout, O. Kaman, Mn-Zn ferrite nanoparticles coated with mesoporous silica as core material for magnetically activated release of therapeutic agents, Journal of Magnetism and Magnetic Materials, submitted.

[25] C. Luna, M. Ilyn, V. Vega, V.M. Prida, J. González, R. Mendoza-Reséndez, Size Distribution and Frustrated Antiferromagnetic Coupling Effects on the Magnetic Behavior of Ultrafine Akaganéite (β-FeOOH) Nanoparticles, Journal of Physical Chemistry C, 118 (2014) 21128-21139. 10.1021/jp5048634.

[26] P.A. Kozin, J.-F. Boily, Proton Binding and Ion Exchange at the Akaganéite/Water Interface, Journal of Physical Chemistry C, 117 (2013) 6409-6419. 10.1021/jp3101046.

[27] F. Mazuel, A. Espinosa, N. Luciani, M. Reffay, R. Le Borgne, L. Motte, K. Desboeufs, A. Michel, T. Pellegrino, Y. Lalatonne, C. Wilhelm, Massive Intracellular Biodegradation of Iron Oxide Nanoparticles Evidenced Magnetically at Single-Endosome and Tissue Levels, ACS Nano, 10 (2016) 7627-7638. 10.1021/acsnano.6b02876.

- Rod-like maghemite particles were prepared by using an akaganeite precursor.
- The oxidation state of Fe was unambiguously determined by Mössbauer spectroscopy.
- At least partial ordering of vacancies in the maghemite structure was evidenced.
- The silica-coated product did not show any cytotoxicity up to 0.42 mmol(Fe)/L